Fire Technology, 2nd Quarter, Vol. 33, No. 2, May/June 1997

Effect of Dissolved Gases on Spray Evaporative Cooling with Water

J. A. Milke, S.C. Tinker, and *M. diMarzo*
University of Maryland, College Park, Maryland

Abstract

An experimental investigation of the effect of nondegassed water used to cool a solid surface is presented. The solid surface is subjected to thermal radiant input from three panels positioned above it. The water is deposited on the surface in the form of a sparse spray with droplets of about 10 μl. Previous experiments with degassed water are compared to a new set of experiments. In addition, the effect of dissolved gases (air) is quantified in terms of the overall transient thermal behavior of the solid. A lower steady-state average temperature is achieved when gases remain in the water. This result suggests that the configuration of the liquid droplets on the surface and the radiant heat input into the droplet are altered by the gas bubbles in the deposited droplet. This information provides insight into fire control mechanisms by automatic sprinkler systems.

Introduction

Evaporative cooling of hot solid surfaces is a desirable heat transfer process in a number of engineering applications. A sparse spray of water deposited on a solid surface removes large amounts of heat due to the high latent heat associated with water evaporation. Industrial uses for spray cooling include quenching molten metals during casting and coating surfaces to form protective finishes. Spray and mist cooling find a variety of uses in the power generation industry, such as the cooling of turbine blades and cooling tower applications. In the area of fire suppression and protection, spray cooling is a primary mechanism of fire extinguishment in many situations, by heat removal from the flaming region or from the burning fuel surface.[1] In addition, a sparse spray may prevent the ignition of fuel close to the burning fuel by cooling the surface of the exposed object. Preventing ignition of neighboring fuels will inhibit fire spread, thereby limiting the fire to the burning object. Such a result is commonly referred to as "fire control," which is the principal objective of automatic sprinkler systems. Yet, previous research efforts related to the fire suppression effects of water sprays have concentrated on the fire extinguishment aspect, with little regard to the control aspect associated with wetting adjacent fuels exposed by the fire.[2]

Surface wetting for fire control purposes reduces the surface temperature of

Keywords: water, spray, cooling, dissolved gases

any fire-exposed fuel. Reduction of the fuel surface temperature by a spray has been studied as a principal extinguishment mechanism.[2] In principle, the mechanics apply to the phenomena involved in fire control, where the droplets reaching the fuel surface remove heat through evaporation. For a spray to effectively prevent ignition of the adjacent fuel, its surface temperature must be kept below the fire point.[2]

Several researchers have focused on the fundamentals of the evaporation of droplets and their cooling effects. Simon and Hsu[3] studied the wetting characteristics of evaporating droplets on various surfaces by recording droplet shape histories at room temperature on copper, lucite, and Teflon® surfaces. Both Toda[4] and Bonacina *et al.*[5] performed early investigations of spray-surface interactions and provided fundamental insight into the uses of mist cooling. Zhang and Yang[6] employed photographic techniques to determine flow patterns in evaporating droplets on glass and copper plates.

The present work constitutes part of a long-range research effort to quantify and develop models for spray cooling hot solid surfaces in a fire environment. In 1989, diMarzo and Evans[7] modeled a single droplet evaporating on a surface with a high thermal conductivity. Subsequently, diMarzo *et al.*[8] developed a theoretical model using boundary element methods to predict the cooling of a semi-infinite solid due to an evaporating droplet. A high and a low thermal-conductivity surface heated from below by conduction were both studied. In 1993, Tartarini *et al.*[9] predicted the transient thermal behavior of a solid caused by the evaporation of a single droplet and proposed a model for the impingement of a sparse spray of droplets. Experimental techniques based on infrared thermography were developed in 1992 to record the evaporation of a droplet on a radiantly heated, semi-infinite solid by diMarzo *et al.*[10] Dawson and diMarzo[11] extended this experimental work to record the effects of a random distribution of droplets (spray) on the surface. In both cases, the solid exhibited low thermal conductivity. Computer models of the evaporation of a single droplet for radiative heat input conditions were contributed most recently by White *et al.*[12] and by Tartarini and diMarzo.[13]

The research presented in this paper expands on Dawson's investigation of the cooling of a solid surface by the evaporation of multiple droplets under radiant heat input. While Dawson used deionized and degassed water in his experiments, the experiments in this work use deionized water that has not been degassed. Therefore, the dissolved gases (air) are at equilibrium with the ambient air at atmospheric conditions. The purposes of this study are to examine both the temporal and spatial behavior of the surface temperature of a low-thermal-conductivity, semi-infinite solid subjected to radiant heat input and to a sparse spray of nondegassed, deionized water; and to quantify the effect of dissolved gases by comparing these results with those from similar experiments using degassed water. By using degassed, deionized water, the experiments are independent of

water quality characteristics. Consequently, use of the degassed, deionized water enhances the reproducibility of the experiments. With reproducible experiments, this study helps develop a basic understanding of one aspect of fire control surface cooling of fire-exposed objects.

Experimental Apparatus

The experimental apparatus is shown in Figure 1. The solid is composed of Macor, a glass-like material. The relevant thermophysical properties of Macor are listed in Table 1. As indicated in the table, Macor exhibits a relatively high emissivity and a relatively low thermal conductivity. A low-thermal-conductivity material is particularly relevant to the issue of limiting fire spread to adjacent

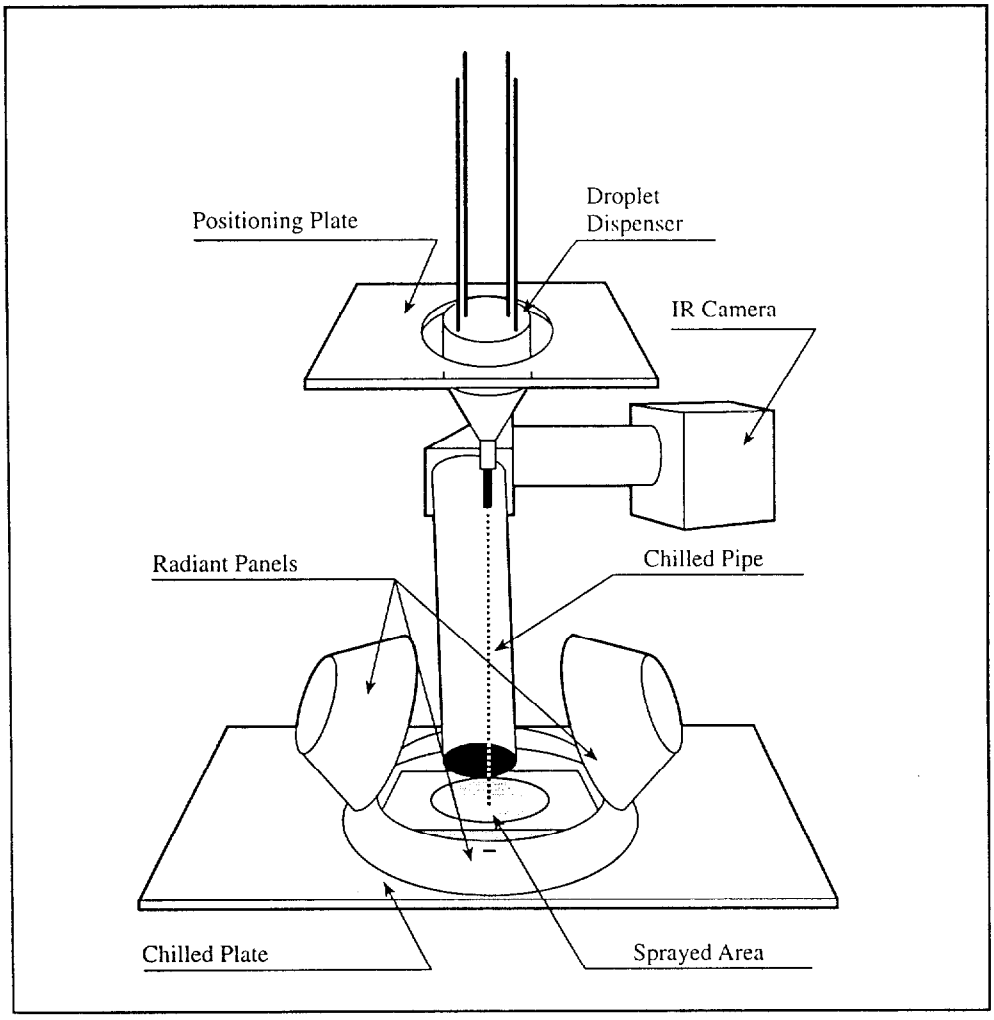

Figure 1. Experimental apparatus.

TABLE 1
Properties of Macor

Density	2,520	kg/m^3
Thermal conductivity	1.297	W/m–K
Specific heat	888.9	J/kg-K
Emissivity	0.84	–

fuel packages as most ordinary combustibles also have a low thermal conductivity. Macor was also selected because of its ability to withstand high thermally induced stresses, resulting in a smooth, crack-free surface. The square Macor tile, with 15.2 cm sides and a thickness of 2.54 cm, is mounted on a chilled plate using a silicone heat sink compound. The purpose of the chilled plate is to hold the lower surface of the tile at a constant temperature of approximately 30°C by circulating cold water through the plate.

Three radiant panels are used to heat the solid surface. Two are above the surface at an angle of 30° and are symmetric to the vertical axis through the center of the tile. The third panel surrounds the perimeter of the tile to heat the sides uniformly. The motivation for using the radiant heat panels—to provide the heat input to the solid surface—is to provide a realistic fire exposure simulation. Each panel is cone-shaped and capable of reaching temperatures in the range of 800°C. The temperatures of the panels are controlled by an Omega CN-7100 digital process controller through a feedback loop from the panels. Power to the panels, which are connected in a delta circuit, is supplied by a 208-volt, three-phase power supply. The radiant flux incident on the sample was not measured because the purpose of the imposed radiant flux was solely to heat the sample to the temperature of interest. The incident flux could be determined analytically by formulating a heat balance on the surface of the sample. Subsequently, the flux delivered by the panels could be determined, assuming an equivalent black body source.

An Inframetrics Model 525 infrared camera, located above the sample, focuses on the solid surface and records its transient thermal behavior. The camera is aimed through a chilled pipe that absorbs stray reflections. The infrared camera detects radiation wavelengths from 8 to 12 m and translates thermal variations of an object into a real-time, gray image. These images are composed of dark shades that represent cool regions and light shades that represent hot regions. The camera records the thermal image of the surface onto 8 mm videotape using a Sony high-resolution VCR. These tapes are stored for subsequent data processing. The camera uses a 0.61 m focal length, close-up lens positioned to view a portion of the surface in the droplet impingement region.

Droplet Size and Distribution

A droplet dispenser hangs vertically above the surface and works with a positioning mechanism to distribute droplets on the surface. The droplet dispenser consists of a tapered cone-shaped, aluminum body with a bored-out central cavity. There is a hole at the bottom of the aluminum body, into which a size 20 IV needle screws. The cavity is continuously fed with water from an open reservoir, which provides the desired static head above the dispenser. A plastic diaphragm and an O-ring seal the cavity at its top. A steel piston rests on top of the diaphragm, while a solenoid-spacer mechanism is fitted to the top of the piston. When the solenoid is energized, it pushes down on the spacer, causing the piston to deflect the diaphragm and eject a droplet from the needle. An average droplet size of 10 μl is obtained with a maximum frequency of 1.0 Hz.

In these spray cooling experiments, attempts are made to distribute the droplets in a random fashion over a circular area of the solid surface. The random distribution of droplets is provided by a positioning mechanism consisting of an aluminum plate with a 25.4 cm hole in the center and three moving solenoid-controlled bumpers that collide with, and impart motion to, the droplet dispenser. The droplet dispenser, which hangs from four cables, swings in the plate hole as it hits the three bumpers. To keep the motion from decaying or falling into a particular pattern, a motorized cam is used to pluck periodically one of the suspension cables.

Figure 2 shows the droplet distribution recorded during a typical experiment. The distribution affects a larger area than that viewed by the infrared camera. The circular region that droplets impinge upon has a radius of approximately 3.3 cm.

The droplet-dispensing mechanism is designed to provide a reproducible droplet distribution that can be described mathematically. The droplet dispenser can move freely within an innermost circle with a radius of 1.8 cm. Beyond this circle, the droplet dispenser motion may be limited by bumpers that move synchronously in the horizontal plane. The innermost position of the bumpers corresponds to a circle with a radius of 1.8 cm, and the outermost position corresponds to a circle with a radius of 3.3 cm. Confined by the motion of the bumpers, the dispenser is never expected to achieve the maximum radial position of 3.3 cm because it is increasingly impeded by the bumpers as it travels farther from the center of the distribution area.

Therefore, a fourth order polynomial function is selected to describe the droplet distribution, namely the fraction of droplets per unit area d at a normalized radius r. With five constants, five boundary conditions are necessary to characterize the droplet distribution:

1. At $r = 0$, $d(r) = 0$ requires that the distribution is proportional to the surface area—that is, no droplets are delivered if $r = 0$.

2. At $r = 0$, $d'(r) = 2$ requires that the distribution is proportional to the surface area—that is, if the surface area is doubled, the number of droplets is also dou-

bled.

3. At $r = h$, $d'(r) = 0$ sets a maximum value for the distribution at the normalized radius h bounding the region of free random motion (the innermost circle) of the droplet dispenser—that is, $h = 0.56$.

4. At $r = 1$, $d = 0$ requires that the outer maximum radial position is never reached—that is, no droplets are delivered beyond the outermost position.

5. $\int_0^1 d\, dr = 1$—that is, normalizes the distribution function.

With these conditions, the function d, describing the droplet distribution, is given as

$$d = 9.15r^4 - 22.64r^3 + 11.49r^2 + 2.00r \tag{1}$$

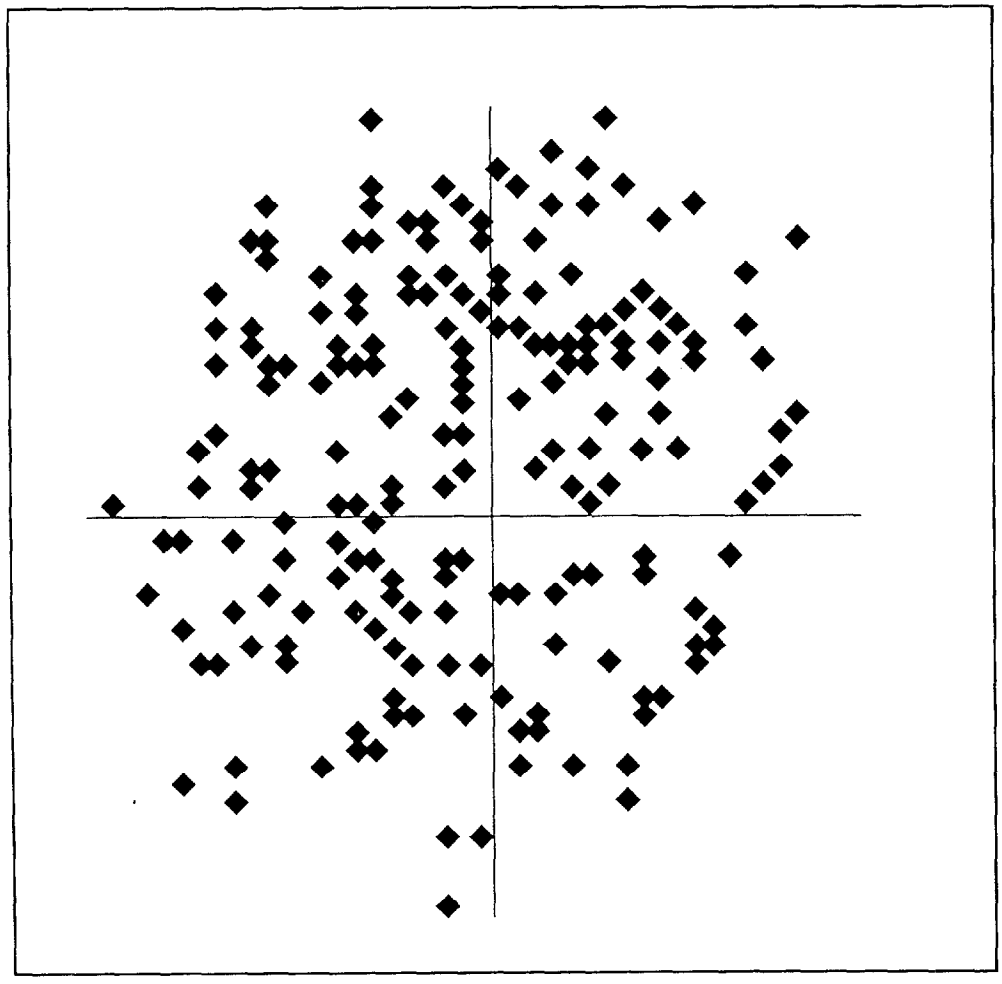

Figure 2. Typical measured droplet distribution.

To check the validity of this result, the integral function is calculated and plotted in Figure 3, along with the measurements. Error bars of the actual data are also shown. The error bars are based on the assumed outermost possible radial position with respect to the outermost droplet. Figure 3 shows that the calculated distribution is in reasonable agreement with the experimental data.

Experimental Procedure

Experiments are conducted with initial surface temperatures of approximately 110°, 130°, 150°, 160°, and 180°C. At each initial surface temperature, three mass fluxes of nondegassed, deionized water are applied, ranging from 0.24 g/m²s to 1.6 g/m²s. These mass fluxes are appreciably less than the 50 to 200 g/m²s typically delivered by automatic sprinkler systems. At these greater mass fluxes, however, the surface is nearing flooding conditions, and less would be learned about the interaction of the droplets with a heated surface. The four lowest initial surface temperatures, 110° to 160°C, correspond to evaporative cooling, while the highest temperature, 180°C, corresponds to full nucleate boiling for the Macor surface.

The basic procedure followed for each experimental session involves the following steps. The Macor surface is cleaned with ethyl alcohol and a soft cloth,

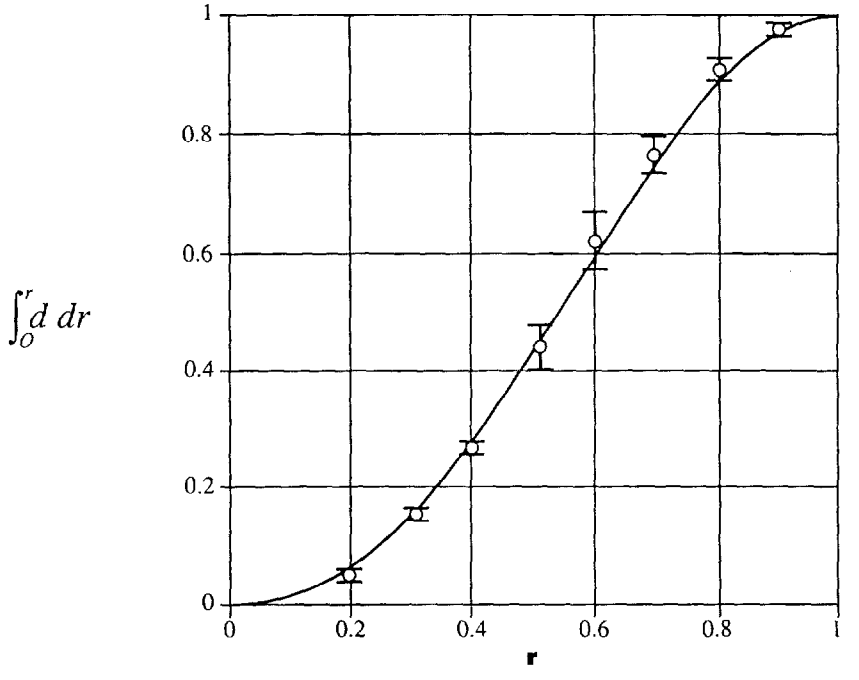

Figure 3. Comparison of the integrated distribution function *d* and the cumulative measured droplet distribution.

lightly rinsed with distilled water, and allowed to dry. The radiant heaters are turned on and heat the sample surface for approximately two hours before the experiments begin. During this time, the solid surface is able to reach a steady-state condition. The temperature of the surface is measured using a type K thermocouple probe. The infrared camera, power supply, and video equipment are also turned on two hours before experimentation to minimize thermal drift. Water is circulated through the chilled plate and chilled pipe. The droplet dispenser is turned on and given 10 to 15 minutes to stabilize at a selected frequency that corresponds to a water mass flux of interest. Once stabilized, 50 droplets are collected in a beaker that is quickly capped to prevent evaporation. The beaker and drops are weighed using a Metler electronic balance, and the volume of a single droplet is determined. Droplet volumes generally ranged from 9 to 11 μl. The range of droplet volumes included in this study is comparable to that provided by an automatic sprinkler system.

After completing the procedures outlined above, an experiment begins for a particular set of conditions. First, the initial surface conditions are recorded, then the droplets impinge upon the heated surface for 25 minutes. During this period, the thermal behavior of the surface is recorded by the infrared camera onto 8 mm videotapes.

Data Processing and Reduction

The data processing and reduction for the experiments follow the same procedure adopted by Dawson[11] in previous spray cooling experiments using degassed water. After completing an experimental run at a given initial surface temperature, the data recorded by the infrared camera are processed. The real-time, gray images recorded by the camera provide two types of information: the transient average temperature of the surface and the spatial temperature distribution on the surface at any instant. Both analyses employ a video digitization system to obtain the gray values from a recorded image. A Matrox MVP-AT frame grabber board is installed in an IBM PC-AT and used to digitize single frames into discrete gray values. One frame is sampled every 30 seconds. Once digitized, each frame can be analyzed pixel by pixel using Imager-AT software linked with user-written source code. For each frame, the infrared intensity scale is calibrated using a temperature-versus-intensity relationship so that shades of gray may be translated into corresponding temperatures.

To determine the transient average surface temperatures, frames are digitized at 30-second intervals of a recorded experimental run. There are 130 shades of gray associated with the infrared intensity levels. Since the temperature range is on the order of 100°C, the temperature resolution is 0.77°C/ gray values. The gray-value of every fifth pixel is used over an image covering a region of 0.046 m by 0.034 m. The average gray values are then converted into a single average surface temperature.

Spatial distributions of the surface temperature at a specific time are obtained by considering each pixel individually in a digitized frame. Each pixel can be associated with a Cartesian coordinate using knowledge about the viewed area of a frame. The gray value for each pixel is converted into a temperature, thus yielding a temperature at a particular location on the surface. Again, every fifth pixel is used. Results are plotted in the form of constant temperature contours. There are pixels 512 in the horizontal direction and 480 in the vertical direction of the total viewed area, respectively.

Results and Discussion

Contour plots of the temperature distribution on the Macor surface are shown in Figures 4a to 4c and 5a to 5c for the indicated initial solid surface temperatures and water mass fluxes. Each sequence of plots shows the surface temperature distribution at three different times: early during the transient period when the surface temperature is close to its initial value; at an intermediate time, before steady-state conditions have been reached; and at or approaching steady-state conditions. Results show very distinct locations where droplets are evaporating on the surface, or have just evaporated from the surface and caused a localized cooling effect. At earlier times, the cooling effect due to evaporating droplets is contained in the local region around the droplet. At later times, more droplets are found on the surface due to the longer evaporation times associated with the decreasing solid surface temperature. At these later times the cooling effect on the surface temperature is attributed to the tendency for several individual droplets to merge. At lower temperatures, isothermal contours are also found near the perimeter of the plot at later times than those found at early times, indicating that the entire surface is cooling. A fluctuation of about ±2°C is associated with these plots, due to electronic noise.

Graphical results of the transient average surface temperature are shown in Figures 6 and 7. The raw data are shown for both the experiments using nondegassed and degassed water,[11] respectively. The general trend apparent in each plot for both the degassed and nondegassed data is the decay of the average surface temperature from its initial value to some steady-state value. Dawson suggested a fit to the transient temperature data of the form

$$T = (T_o - T_s)e^{-at} + T_s \tag{2}$$

which is used to curve-fit all the data representing the transient behavior of the average solid surface temperature. The deviation of the data points from a smooth decay occurs because of the nature of the data acquisition process. Because only a portion of the sprayed area is viewed and averaged at any instant, the number of droplets that can be seen may be different than at other instants, resulting in oscillations of the average surface temperature.

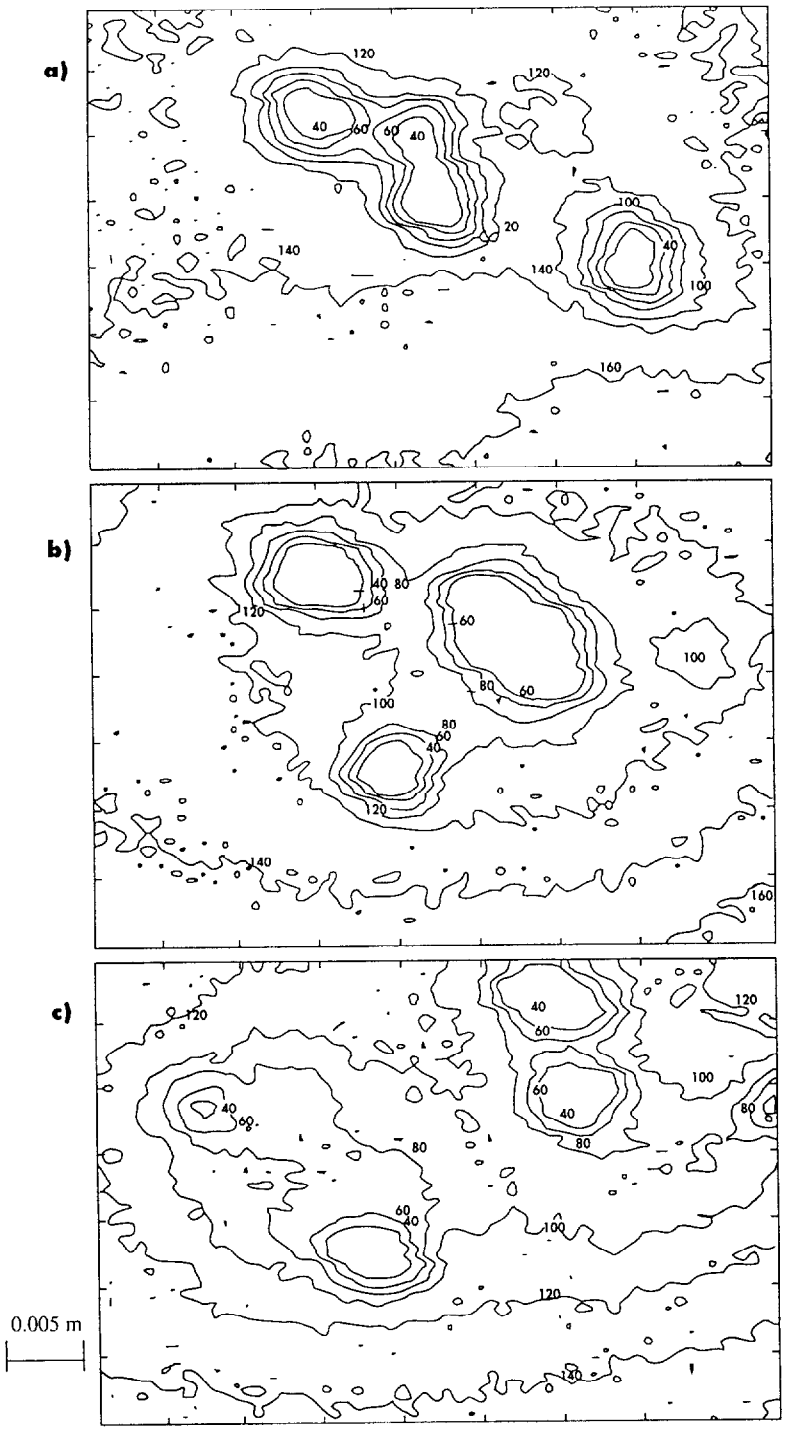

Figure 4. Surface temperature contour plot for T_o=151°C and G=0.96 g/m²s (a: t=30 s; b: t=300 s; c: t=600 s).

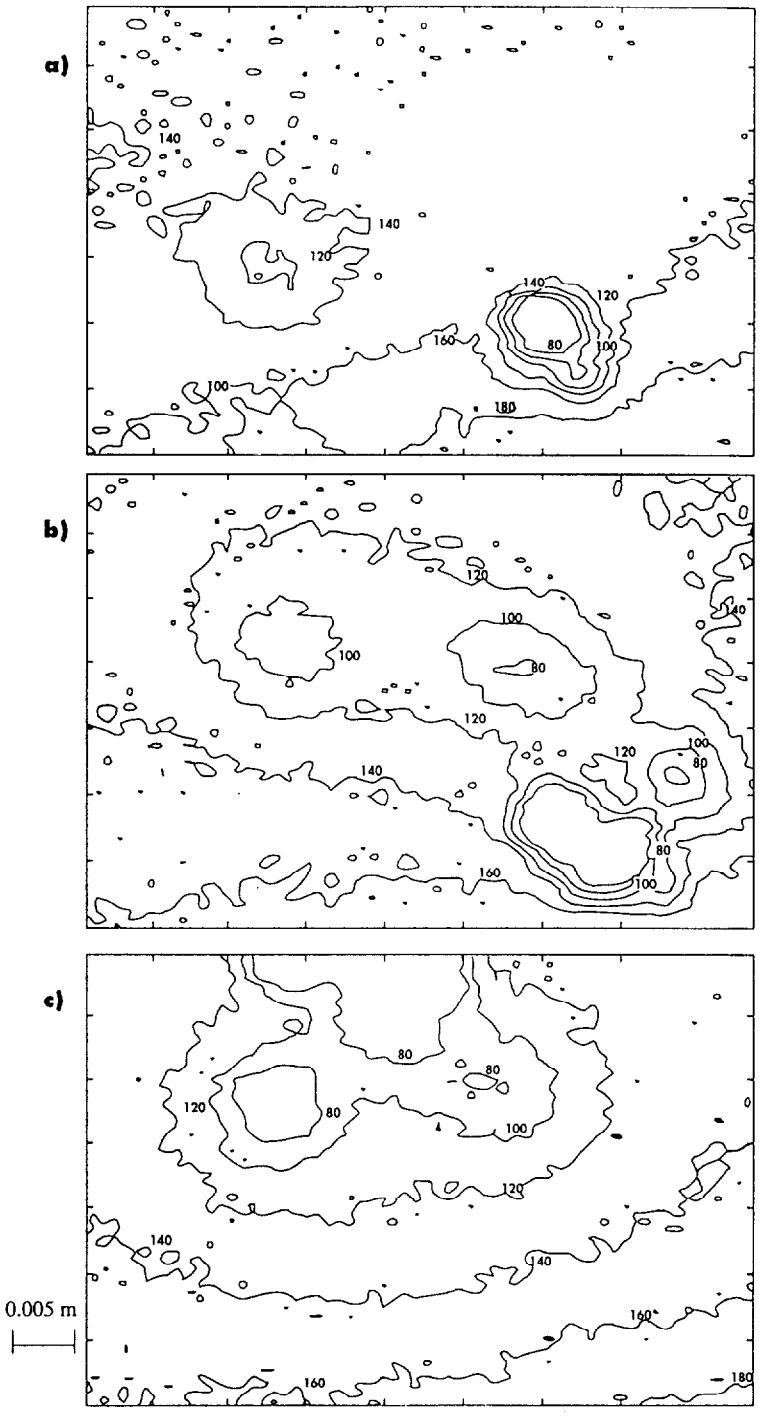

Figure 5. Surface temperature contour plot for T_o=162° and G=0.97 gm²s (a: t=30 s; b: t=300 s; c: t=600 s).

Examination of these results suggests that the dissolved gases enhance the heat transfer from the surface by decreasing the radiant input to achieve a lower steady-state temperature. To quantify this effect, the variation in the final steady-state temperature must be related to the temperature excursion present in the degassed water results. Two major effects must be included in the characterization of a given transient: ΔT, the solid surface temperature drop, and θ, the difference between the solid surface temperature at the onset of nucleate boiling for degassed water and the actual initial solid surface temperature. θ serves as a physically significant reference temperature. ΔT and θ are related to the water mass flux and to the radiant heat input, respectively.

An independent variable can be identified as the ratio of the temperature drop ΔT and the initial temperature difference θ while retaining the temperature variation as the dependent variable. Table 2 lists the actual numerical values for each of the variables. One trend indicated by the ratio is that the effect of dissolved gases becomes negligible as the values of the ratio $\Delta T/\theta$ increases. The ratio is greatest for large reductions in temperature and for initial solid surface temperatures near the onset of nucleate boiling conditions for degassed water. These conditions are most likely in the context of fire control. Because the effect of the dissolved gases is negligible for this situation, the evaporative cooling processes associated with fire safety applications are independent of the presence of dis-

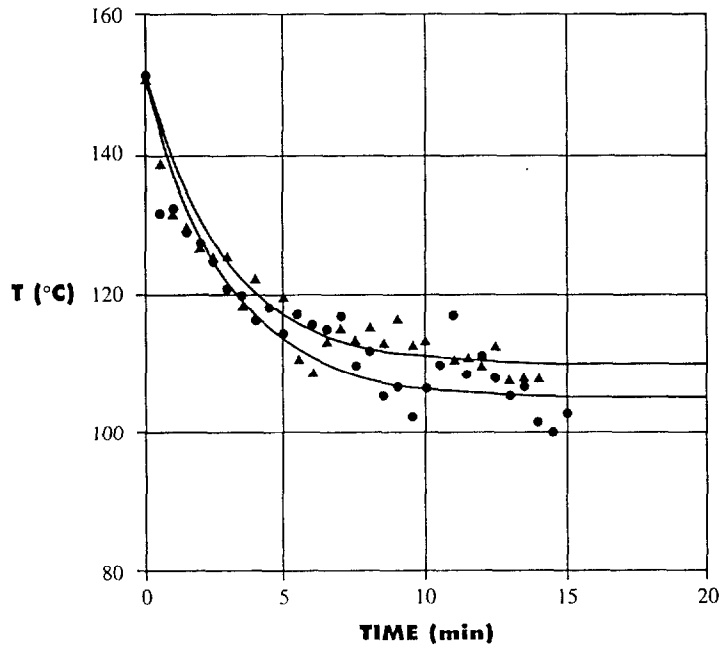

Figure 6. Transient average surface temperature for T_o=151°C and G=0.96 g/m²s (●: nondegassed; fit: $T=41e^{-0.35t}+110$; ▲: degassed, fit: $T=46e^{-0.34t}+105$).

TABLE 2
Gassed-Degassed Water Comparison

Gassed ΔT	Degassed θ	Result $\Delta T/\theta$	Comparison $T_s - T_s^*$
61	12	5.1	4
41	12	3.4	5
25 (29)[a]	32	0.78 (0.90)	8 (4)
85	1	85	1
40	1	40	0
77	−19[b]	–	2

[a] The mass flux for the degassed water is 0.5 g/m²s while the mass flux for the gassed water is 0.57 g/m²s. The quantities in parentheses are prorated to correct for this mass flux discrepancy.

[b] For degassed water, the initial solid surface temperature at the onset of boiling is 163°C. A negative value of O indicates that the nucleate boiling point is present. O of −19°C corresponds to an initial solid surface temperature of 182°C.

solved gases. Consequently, research results with degassed water presented in this paper are also applicable to situations where nondegassed water is used for fire control, as is the case with water discharged from automatic sprinkler systems.

These conclusions do not apply for temperatures of the solid surface, where nucleate boiling is observed (that is, for negative values of θ). The nature of the vaporization phenomena in nucleate boiling is based on a completely different heat transfer mechanism, and an extension of the evaporative results or trends is not justified.

Conclusions

The spatial and temporal behavior of the transient surface temperature of a radiantly heated semi-infinite solid cooled by a sparse spray of nondegassed water can be recorded and analyzed using a data acquisition system that uses digital image analysis and infrared thermography. The transient thermal behavior is investigated over a range of different initial surface temperatures and water mass fluxes. The data acquisition system is able to provide information on both the spatial and temporal behavior of the solid in the form of contour plots and transient average temperature plots, respectively.

Contour plots provide a qualitative description of the surface at any instant in

time. Results indicate that localized cooling in the region of droplets occurs during the initial impingement of the sparse spray on the surface. Later, effects of the droplets tend to merge, and the average temperature on the surface decreases. More droplets are also found on the surface later due to the longer evaporation times associated with the lower surface temperatures.

Transient surface temperature results are compared to those results obtained from experiments using degassed water. In both cases, the surface exhibits an exponential cooling from its initial temperature to a steady-state condition. For larger values of the ratio $\Delta T/\theta$ (the ratio of the temperature change to a reference temperature), only a slight difference in the surface cooling is observed between application of nondegassed and degassed water. Conversely, for low values of the $\Delta T/\theta$ ratio, these experiments indicate that the dissolved gases enhance the cooling process by reducing the incoming radiant input. Because nondegassed water has cooling capabilities superior to those of degassed water, experimental investigations using degassed water to evaluate surface wetting of combustibles exposed to fire will be conservative by underestimating the effect of the applied water mass flux.

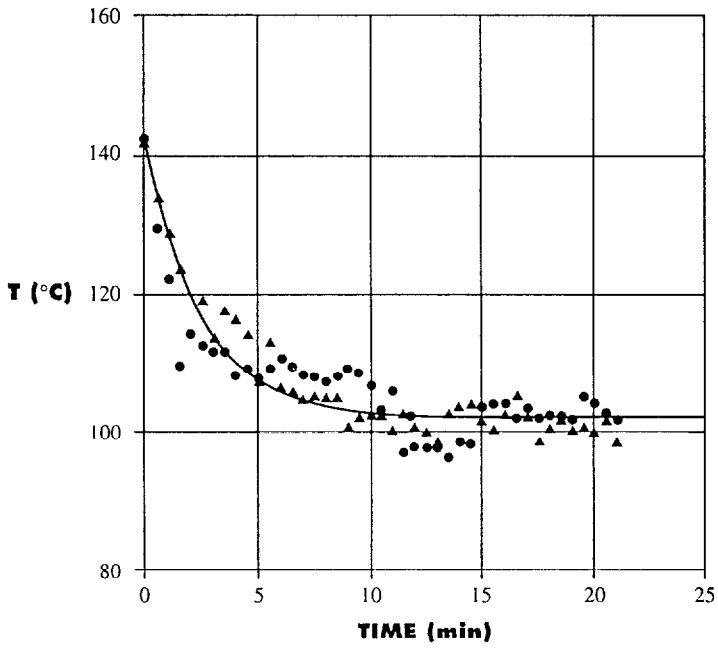

Figure 7. Transient average surface temperature for T_o=162°C and G=0.97 g/m²s (●: nondegassed; ▲: degassed, fit: $T=40e^{-0.401t}+122$ for both sets of data).

Acknowledgments

This research was sponsored by a grant from the Building and Fire Research Laboratory of the National Institute of Standards and Technology.

References

1. Rasbash, D. J., "The Extinction of Fire with Plain Water: A Review," *Fire Safety Science—Proceedings of First International Symposium*, Int. Association of Fire Safety Science, 1986, pp. 1,145–1,163.

2. Rasbash, D. J., "The Extinction of Fires by Water Sprays," *Fire Research Abstracts and Reviews*, Vol. 4 (1962), pp. 28–52.

3. Simon, F., Hsu, Y. Y., "Wetting Dynamics of Evaporating Drops on Various Surfaces," *NASA Technical Memo, NASA TM X-67913* (1971).

4. Toda, S., "A Study of Mist Cooling," First Report: Investigation of Mist Cooling. *J. of Heat Transfer*, Japanese Research, Volume. 1 (1972), p. 39–50.

5. Bonacina, C., Del Giudice, S., Comini, G., "Dropwise Evaporation," *Journal of Heat Transfer*, Vol. 101 (1979), pp. 441–446.

6. Zhang, N., Yang, W. J., "Natural Convection in Evaporating Minute Drops," *J. of Heat Transfer*, Vol. 104 (1982), pp. 656–662.

7. diMarzo, M., Evans, D., "Evaporation of a Water Droplet Deposited on a Hot High Conductivity Solid Surface," *Journal of Heat Transfer*, Vol. 111 (1989), pp. 210–213.

8. diMarzo, M., Tartarini, P., Liao, Y., Evans, D., Baum, H., "Evaporative Cooling Due to a Gently Deposited Droplet," *International Journal of Heat and Mass Transfer, Vol* 36 (1993), pp. 4,133–4,139.

9. Tartarini, P., Liao, Y., diMarzo, M., "Numerical Simulation of Multi-Droplet Evaporative Cooling," *Heat and Technology*, Vol. 11 (1993), pp. 98–107

10. diMarzo, M., Kidder, C. H., Tartarini, P., "Infrared Thermography of Dropwise Evaporative Cooling of a Semi-Infinite Solid Subjected to Radiant Heat Input," *Experimental Heat Transfer*, Vol. 5 (1992), p. 101–104.

11. Dawson, H., diMarzo, M., "Multi-Droplet Evaporative Cooling," Experimental results. AIChE Symposium Series, Vol. 89 (1993), pp. 26–35.

12. White, G., Tinker, S., diMarzo, M., "Modelling of Dropwise Evaporative Cooling on a Semi-Infinite Solid Subjected to Radiant Heat Input," *Fire Safety Science—Proceedings of the 4th International Symposium*, ed. T. Kashiwagi, International Association of Fire Safety Science (1994), pp. 217–228.

13. Tartarini, P., diMarzo, M., "Dropwise Evaporative Cooling in Radiative Field," *Proceedings of the 10th International Heat Transfer Conference*, ed. G.F. Hewitt, Vol. 6 (1994), pp. 277–282.

Nomenclature

a	constant
d	droplet distribution function
G	droplet mass flux
h	maximum normalized radius of free random motion of the droplet distributor
r	normalized radius (with respect to its maximum possible value of 3.3 cm)
T	average solid surface temperature
T_o	initial solid surface temperature
T_s	final steady state average solid surface temperature
t	time

Greek

ΔT	solid surface temperature drop, $T_o - T_s$
θ	difference between the solid surface temperature at the onset of nucleate boiling for degassed water (~ 163 °C) and the actual initial solid surface temperature

Superscripts

*	identifier of properties for degassed water
'	identifier of the first derivative with respect to r